Pharmaceutical Research (2022) 39:2607–2620
https://doi.org/10.1007/s11095-022-03359-y

ORIGINAL RESEARCH ARTICLE

Optimization of Initial Drug Distribution in Spherical Capsules for Personalized Release

Ankur Jain[1] · Kamesh Subbarao[1] · Sean McGinty[2,3] · Giuseppe Pontrelli[4]

Received: 2 June 2022 / Accepted: 4 August 2022 / Published online: 7 September 2022

Abstract

Objective Customization of the rate of drug delivered based on individual patient requirements is of paramount importance in the design of drug delivery devices. Advances in manufacturing may enable multilayer drug delivery devices with different initial drug distributions in each layer. However, a robust mathematical understanding of how to optimize such capabilities is critically needed. The objective of this work is to determine the initial drug distribution needed in a spherical drug delivery device such as a capsule in order to obtain a desired drug release profile.

Methods This optimization problem is posed as an inverse mass transfer problem, and optimization is carried out using the solution of the forward problem. Both non-erodible and erodible multilayer spheres are analyzed. Cases with polynomial forms of initial drug distribution are also analyzed. Optimization is also carried out for a case where an initial burst in drug release rate is desired, followed by a constant drug release rate.

Results More than 60% reduction in root-mean-square deviation of the actual drug release rate from the ideal constant drug release rate is reported. Typically, the optimized initial drug distribution in these cases prevents or minimizes large drug release rate at early times, leading to a much more uniform drug release overall.

Conclusions Results demonstrate potential for obtaining a desired drug delivery profile over time by carefully engineering the drug distribution in the drug delivery device. These results may help engineer devices that offer customized drug delivery by combining advanced manufacturing with mathematical optimization.

Keywords controlled release · drug delivery · inverse problems · optimization

Nomenclature

A	Initial (erodible case) or fixed (non-erodible case) radius (m).
B	Rate of erosion of the erodible sphere (m s^{-1}).
c	Concentration (mol m^{-3}).
D	Diffusion coefficient (m^2 s^{-1}).
J	Order of the polynomial function.
M	Number of layers.
M_{total}	Total drug amount (mol).
q_a	Actual drug release rate (mol s^{-1}).
q_d	Desired drug release rate (mol s^{-1}).
R	Radius of erodible sphere as a function of time (m).
r	Radial coordinate (m).
t	Time (s).
λ	Non-dimensional eigenvalue.
θ	Non-dimensional concentration, $\theta = c/c_{ref.}$
τ	Non-dimensional time, $\tau = Dt/A^2$
ξ	Non-dimensional radial coordinate, $\xi = r/A$

Subscripts

in	Initial
ref	Reference
m	Layer number

✉ Ankur Jain
jaina@uta.edu

[1] Mechanical and Aerospace Engineering Department, University of Texas at Arlington, 500 W First St, Rm 211, Arlington, TX 76019, USA

[2] Division of Biomedical Engineering, University of Glasgow, Glasgow, UK

[3] Glasgow Computational Engineering Centre, University of Glasgow, Glasgow, UK

[4] Istituto per le Applicazioni del Calcolo – CNR, Via dei Taurini 19, 00185 Rome, Italy

Introduction

Drug delivery devices such as tablets/capsules [1], stents [2] and transdermal patches [3] are commonplace in the clinic [4, 5]. In designing such devices, the drug release profile (i.e., the rate at which the initial drug loaded is released as a function of time) is usually of primary consideration [1, 6]. In most applications, it is desirable to maintain local drug concentrations within some therapeutic range for a defined period of time. However, depending on the local physiological environment, spells of under- or -overexposure may occur if the drug release rate is not tailored appropriately. It is noteworthy that most drugs are presented as immediate release formulations, which result in a rapid initial increase in systemic drug concentrations, which can lead to several undesirable effects [7]. One example is drug-filled PLGA particles which usually involve an initial burst of drug, resulting from fabrication where the drug primarily resides on the particle surface [7]. As discussed in [7], this can lead to toxicity, rapid depletion of the drug within the particle and complications in redosing. A constant drug release rate (so-called zero-order release) can help to alleviate this concern by minimizing variation in local drug concentrations [8]. However, zero-order release is difficult to achieve in practice, particularly when the drug is presented in a form that permits rapid dissolution [9]. In such cases, diffusion typically governs the rate of drug release, and first-order release kinetics are usually observed, giving rise to a variable drug-release rate. Despite the aforementioned advantages of zero-order release, in some situations, an initial burst of drug may be desirable. For example, in the case of drug-eluting stents, it has been reported that the drug release should be programmed to quickly bind to and saturate specific receptors on target cells, before providing sustained release to match declining levels of bound drug at later times [10].

Drug delivery tablets are traditionally manufactured by mixing the Active Pharmaceutical Ingredient (API) in an inactive chemical, known as the excipient, such as Polyvinyl Alcohol (PVA), along with other minor ingredients for binding, strength and stability [11]. While most tablets are designed to contain uniform concentration of a single drug, some work also exists on bilayer or multilayer tablets, wherein each layer contains uniform concentration of a different drug [12, 13]. More recently, 3D printing of tablets, often referred to as printlets, has been heavily investigated [14–17]. 3D printing is much slower than traditional manufacturing, but may offer the capability of customization according to individual patient needs. 3D printing of tablets has been reported using techniques such as Fused Filament Fabrication (FFF) [14], selective laser sintering [15], stereolithography [16] and binder jetting [17]. Using these techniques, it may be possible to print tablets in which the drug concentration varies between and/or within the layers. Advanced manufacturing methods may also help print other multilayer drug delivery devices, such as stents, transdermal patches, etc.

Experimental investigation of drug release characteristics from drug delivery devices, especially *in vivo*, is often time-consuming and expensive. The number of design features that can be explored experimentally is often limited, and therefore, an accurate design of experiments is critical. In light of this, theoretical modeling of drug release plays an important role in developing a fundamental understanding of the factors that influence drug delivery, which in turn may help maximize the benefits of measurements [1, 18]. Theoretical modeling of drug release is based on solving the underlying conservation equations, often written in the form of transient partial differential equations, subject to appropriate boundary and initial conditions [1, 19, 20]. While most of the literature accounts only for diffusion as the dominant transport mechanism, advective transport due to fluid flow, such as radial pressure gradient driven plasma flow in an artery [21, 22], as well as drug absorption within the capsule prior to release [6] have also been accounted for. Other factors, such as surface or bulk erosion of the capsule [23, 24], dissolution [25], multi-drug diffusion [26] and drug binding after release [27] have also been modeled.

Most of the theoretical work outlined above focuses on determining the drug release profile for a given set of input parameters such as geometry and diffusion coefficients. In contrast, the inverse problem, i.e., to determine the optimal design of the drug delivery device that produces a desirable drug release profile, has received relatively less attention. For example, while the nature of diffusion makes it inherently impossible to obtain a constant drug release rate from a uniformly loaded drug delivery device, in the case of a multilayer drug delivery device, it may be possible to configure the drug concentration in each layer in such a way as to obtain a drug release rate that is as close to a constant, or indeed any desired function of time, as possible. In practice, the underlying physics likely makes it impossible to achieve precisely the desired drug delivery rate, however, it is, in principle, possible to seek an initial drug distribution that minimizes the deviation from the desirable drug release rate over the delivery period. Mathematical modeling and optimization provide the required tools in pursuit of this goal. Such design optimization, coupled with advances in multilayer manufacturing methods, may result in customized drug delivery devices, in which, the drug release profile is tailored to the local environment and needs of the individual patient.

In general, optimization methods have not been applied sufficiently for drug delivery problems, especially when compared to other engineering problems [28]. The impact of the initial drug distribution on drug delivery characteristics in a flat, slab-shaped device has been recognized [29, 30], and optimization of the initial drug distribution towards a desirable delivery profile has been carried out [31, 32]. However, these papers do not sufficiently account for the important and practical phenomenon of erosion, except as a limiting case with zero diffusion [29]. In practice, erosion and diffusion occur simultaneously to determine drug delivery characteristics of an erodible drug delivery device [23]. Moreover, these papers are not directly applicable to spherical drug delivery devices, such as capsules.

This paper presents inverse analysis and optimization of diffusion-based drug delivery from a spherical drug delivery device, such as a capsule or a tablet. Both non-erodible and surface-erodible drug delivery devices are considered. The problem is cast in the form of an inverse mass transfer optimization problem, with the goal of determining an initial drug distribution that results in a drug delivery profile that is as close as possible to a desired profile. Polynomial or discrete multilayer functions for the initial drug distribution are considered, and surface erosion is accounted for. Optimization is carried out for cases where zero-order release is desired, as well as ones with a desired initial burst. It is shown that optimization of initial drug distribution in each layer of a multilayer spherical drug delivery device results in a drug delivery profile that is much closer to a desired profile than the baseline case of uniform drug distribution.

Problem Definition and Derivation of Solution

Spherical Layered Non-Eroding Capsule

Consider the problem of drug delivery from a spherical capsule of fixed radius A containing drug of total mass M_{total}. A multilayer capsule, as shown schematically in Fig. 1(a), is considered first, which can be manufactured through layer-by-layer deposition around a solid core. The initial drug distribution of each layer may be designed to be different, resulting in a discrete initial drug distribution. For an M layer capsule, this may be mathematically expressed as $c = c_{in,m}$ at $t = 0$ for $R_{m-1} < r < R_m$ $(m = 1,...M)$ where R_{m-1} and R_m are the inner and outer radii of the m^{th} layer. Note that $R_0 = 0$ and $R_M = A$. The radii may be equally spaced, but not necessarily so. The case of continuous initial drug distribution, say, $c = c_0(r)$ at $t = 0$ for $0 < r < A$ (Fig. 1(b)) is considered in a subsequent sub-section.

Diffusion of the initial drug distribution to the outer surface of the sphere, followed by convective transport at the surface, results in release of the drug to the surrounding medium. Drug absorption within the sphere is neglected, and, thus, in principle, all of the drug is released over time. The timescale for dissolution of drug is assumed to be much shorter than for diffusion, so that the entire drug distribution in the sphere begins to diffuse immediately at the initial time. It is assumed that each layer consists of the same excipient such that each layer has the same diffusion coefficient that remains invariant with time. Erosion of the sphere over time is neglected here, so that the outer radius remains fixed. The bioerodible case is considered in the next sub-section. Assuming a circumferentially symmetric sphere with drug loading varying only in the radial direction, drug diffusion occurs only in the radial direction.

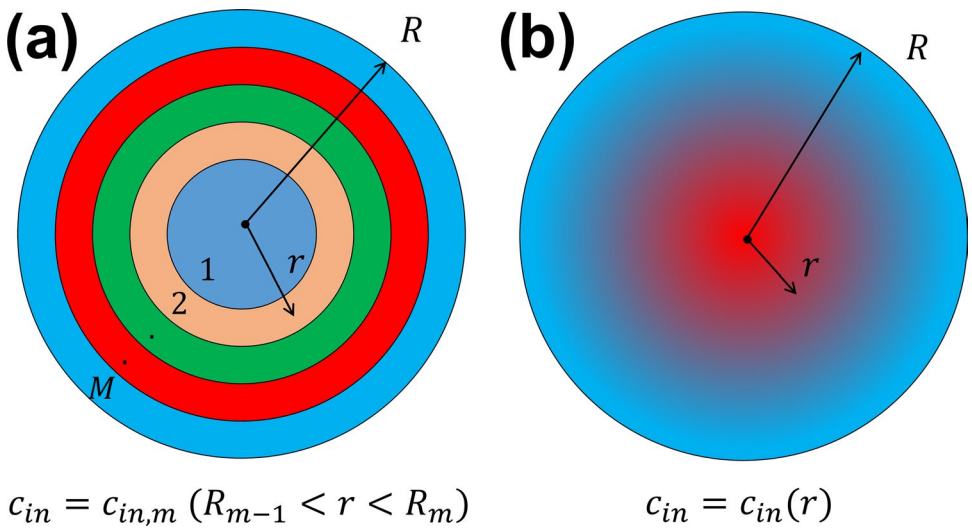

Fig. 1 Schematic of a spherical capsule of radius R with (a) discrete (multilayer), or (b) continuous initial drug concentration.

The release medium surrounding the capsule is assumed to be an infinite sink, which is appropriate when the capsule is immersed in a relatively large volume of fluid.

Under these assumptions, for a desired rate of drug release as a function of time, $q_d(t)$, the interest is in determining the initial drug distribution which results in an actual drug release rate $q_a(t)$ that is identical, or as close as possible to the desired rate $q_d(t)$. In many cases, a uniform rate of drug delivery is desired, i.e., a flat q_d curve over the period of drug delivery. In some cases, an initial burst in drug delivery may also be desirable. From a theoretical mass transfer perspective, this is an inverse mass transfer optimization problem. In principle, there may not exist any initial drug distribution, for which, $q_a(t)$ exactly matches $q_d(t)$. Instead, one must seek to optimize the initial drug distribution, for example, by minimizing the root-mean-square deviation between the actual $q_a(t)$ and the desired $q_d(t)$. The forward problem is first defined and solved, i.e., an expression for $q_a(t)$, given an initial drug distribution, is derived. Based on this solution, the optimization problem is then defined and solved.

Based on the assumptions described above, the mass conservation equation governing the present problem within the sphere and up to a total release time t_{total} may be written as

$$\frac{\partial c}{\partial t} = \frac{D}{r^2}\frac{\partial}{\partial r}\left(r^2\frac{\partial c}{\partial r}\right) \qquad 0 < r < A; \qquad 0 < t < t_{total} \tag{1}$$

along with boundary and initial conditions given by

$$\frac{\partial c}{\partial r} = 0 \qquad r = 0 \tag{2}$$

$$c = 0 \qquad r = A \tag{3}$$

$$c = c_{in,m} \qquad R_{m-1} < r < R_m \ (m = 1, 2 \ldots M); \quad t = 0 \tag{4}$$

Once this problem is solved, the actual drug release profile is given by

$$q_a(t) = -D\left(\frac{\partial c}{\partial r}\right)_{r=A} \cdot 4\pi A^2 \tag{5}$$

This problem is first non-dimensionalized as follows:

$$\theta = \frac{c}{c_{ref}}, \qquad \xi = \frac{r}{A}, \qquad \tau = \frac{Dt}{A^2} \tag{6}$$

where the reference concentration c_{ref} is chosen to be $c_{ref} = \frac{M_{total}}{\frac{4}{3}\pi A^3}$, which is the concentration if the entire drug amount M_{total} was distributed uniformly within the capsule. Accordingly, the non-dimensional governing equations are

$$\frac{\partial \theta}{\partial \tau} = \frac{1}{\xi^2}\frac{\partial}{\partial \xi}\left(\xi^2\frac{\partial \theta}{\partial \xi}\right) \qquad 0 < \xi < 1; \qquad 0 < \tau < \tau_{total} \tag{7}$$

subject to

$$\frac{\partial \theta}{\partial \xi} = 0 \qquad \xi = 0 \tag{8}$$

$$\theta = 0 \qquad \xi = 1 \tag{9}$$

$$\theta = \theta_{in,m} \qquad \gamma_{m-1} < \xi < \gamma_m \ (m = 1, 2 \ldots M); \qquad \tau = 0 \tag{10}$$

where $\theta_{in,m} = \frac{c_{in,m}}{c_{ref}}$ are the non-dimensional initial drug concentrations in each layer, $\gamma_m = \frac{R_m}{A}$ are the radii of the layers, and $\tau_{total} = \frac{Dt_{total}}{A^2}$ is the total non-dimensional drug release time. In this framework of non-dimensionalization, the non-dimensional drug delivery profile may be defined as $\overline{q}_a(\tau) = \frac{q_a(t)A^2}{3DM_{total}} = -\left(\frac{\partial \theta}{\partial \xi}\right)_{\xi=1}$.

Equations (7)–(10) represent a forward mass transfer problem, in which an initial drug distribution $\theta_{in,\,m}$ is given and the resulting non-dimensional drug delivery profile, $\overline{q}_a(\tau) = -\left(\frac{\partial \theta}{\partial \xi}\right)_{\xi=1}$ is to be determined. This problem is solved first, because the solution of this direct problem provides the theoretical basis for solving the inverse problem. A straightforward solution for eqs. (7)–(10) may be obtained using the method of separation of variables as [20]

$$\theta(\xi, \tau) = \sum_{n=1}^{\infty} A_n \frac{\sin\left(\lambda_n \xi\right)}{\xi} \exp\left(-\lambda_n^2 \tau\right) \tag{11}$$

where $\lambda_n = n\pi$ $(n = 1, 2, 3\ldots)$ are the eigenvalues and, based on the principle of orthogonality, coefficients A_n are given by

$$A_n = 2\sum_{m=1}^{M} \frac{\theta_{in,m}}{\lambda_n^2}\left[\sin\left(\lambda_n\gamma_m\right) - \lambda_n\gamma_m\cos\left(\lambda_n\gamma_m\right) - \sin\left(\lambda_n\gamma_{m-1}\right) + \lambda_n\gamma_{m-1}\cos\left(\lambda_n\gamma_{m-1}\right)\right] \tag{12}$$

Subsequently, the rate of drug delivery into the release medium as a function of time is given by

$$\overline{q}_a(\tau) = -\left(\frac{\partial \theta}{\partial \xi}\right)_{\xi=1} = -\sum_{n=1}^{\infty} A_n\lambda_n\cos\left(n\pi\right)\exp\left(-\lambda_n^2\tau\right) \tag{13}$$

For a sphere in which each layer is loaded with the same concentration, $\overline{q}_a(\tau)$ will be largest at small times, when drug concentration gradient at the surface is the highest. As drug is released and drug amount within the capsule reduces, $\overline{q}_a(\tau)$ decreases at large times. The precise nature of $\overline{q}_a(\tau)$ depends on the initial drug distribution in each layer, which appears in eq. (13) within the A_n terms.

Now, the problem of determining the initial drug distribution that results in a $\overline{q}_a(\tau)$ that is as close as possible to a desired $\overline{q}_d(\tau)$ may be posed as an optimization problem. The goal is to determine the initial drug concentrations in each layer, $\theta_{in,\ m}$, so as to minimize the root-mean-square deviation between $\overline{q}_a(\tau)$ and $\overline{q}_d(\tau)$ over a time period, i.e.,

$$\text{minimize } S = \sqrt{\frac{1}{i_{total}} \sum_{i=1}^{i_{total}} \left[\overline{q}_a(\tau_i) - \overline{q}_d(\tau_i)\right]^2} \tag{14}$$

$$\text{subject to } \sum_{m=1}^{M} \theta_{in,m} \frac{\gamma_m^3 - \gamma_{m-1}^3}{3} = \frac{1}{3} \tag{15}$$

$$\text{subject to } \theta_{in,m} \geq 0 \ \ m = 1, 2..., M \tag{16}$$

where τ_i are discrete times in a certain time duration $0 < \tau < \tau_{total}$ that are used to determine S, the root-mean-square (RMS) error, i_{total} is the total number of times considered and $\overline{q}_d(\tau)$ is the non-dimensional desired drug delivery rate in this time period. The constraint given in eq. (15) represents the requirement to load a fixed total mass M_{total} of the drug in the sphere. The constraint given in eq. (16) represents the requirement for the initial drug concentration in each layer to be positive, since negative drug concentration is not meaningful. Finally, the total time in which to consider this problem may be taken to be the diffusive timescale corresponding to the sphere radius, given by $t_{total} = \frac{A^2}{4D}$, and therefore, in the non-dimensional problem, $\tau_{total} = 0.25$. This problem has been formulated in a general manner, and can be solved for any desired drug delivery rate $\overline{q}_d(\tau)$. For example, a constant drug delivery rate is often desirable, in which case, it can be shown that $\overline{q}_d = \frac{4}{3}$. Further, the general nature of this problem statement facilitates analysis of any value of M, depending on the maximum number of layers that can be reliably manufactured.

A similar problem for a surface-erodible sphere is defined next.

Spherical Layered Surface-Erodible Capsule

This section considers the optimization of initial drug distribution in a multilayer spherical capsule assumed to be undergoing linear surface erosion, so that the sphere radius reduces as $R(t) = A - Bt$, where A is the initial radius and B is the rate of erosion. The assumption of linear surface erosion is supported by theoretical modeling [33] as well as experimental observations [34]. It is assumed that D remains unaffected by the erosion process. In the context of this problem, the interest is to understand how the optimal drug distribution may deviate from the results for the non-erodible sphere.

The direct problem of predicting the rate of drug delivery from a linear single-layer surface-erodible sphere has been recently solved [23]. Using a coordinate transformation, the non-dimensional transient concentration distribution for a given initial drug distribution has been shown to be [23] where

$$\theta(\xi, \tau) = \left(1 - \overline{B}\tau\right)^{-1/2} \exp\left(\frac{\xi^2 \overline{B}}{4\left(1 - \overline{B}\tau\right)}\right) \sum_{n=1}^{\infty} \frac{A_n \left(1 - \overline{B}\tau\right)}{\xi} \sin\left(\frac{\lambda_n \xi}{1 - \overline{B}\tau}\right) \exp\left(-\frac{\lambda_n^2 \tau}{1 - \overline{B}\tau}\right) \tag{17}$$

$$A_n = 2 \sum_{m=1}^{M} \theta_{in,m} \int_{\gamma_{m-1}}^{\gamma_m} \xi^* \sin\left(\lambda_n \xi^*\right) \exp\left(-\frac{\xi^{*2} \overline{B}}{4}\right) d\xi^* \tag{18}$$

Here, $\overline{B} = AB/D$ is the non-dimensional rate of erosion. Eigenvalues λ_n are the same as the previous sub-section. Note that while the previous work [23] considered the case of the initial distribution given by a continuous function, eq. (18) represents an adaptation for the present case, in which the initial distribution is discrete.

As a result, the non-dimensional rate of drug delivered is given by

$$\overline{q}_a(\tau) = -\left(\frac{\partial \theta}{\partial \xi}\right)_{\xi = 1 - \overline{B}\tau} \left(1 - \overline{B}\tau\right)^2 = \left(1 - \overline{B}\tau\right)^{-1/2} \exp\left(\frac{\overline{B}\left(1 - \overline{B}\tau\right)}{4}\right) \sum_{n=1}^{\infty} A_n \lambda_n \cos\left(\lambda_n\right) \exp\left(-\frac{\lambda_n^2 \tau}{1 - \overline{B}\tau}\right) \tag{19}$$

As expected, for $\overline{B} = 0$, eqs. (17)–(19) reduce to corresponding results for the non-erodible sphere discussed in section 2.1. Moreover, the constraints related to fixed total drug mass, given by eq. (15) and positive initial drug distribution in each layer, given by eq. (16) continue to apply for the surface-erodible case. Therefore, optimization for this case of discrete initial drug distribution in a surface-erodible sphere may be carried out based on eqs. (14), (15) and (16), where $\overline{q}_a$ is given by eq. (19).

Note that since the sphere erodes at a uniform rate, the entire sphere vanishes when $R(t)=0$, i.e., $t=A/B$, and therefore, the time period in which drug must be delivered is given by $\tau_{total} = 1/\overline{B}$. Therefore, the ideal, constant rate of drug delivery in this time period is given by $\overline{q}_d = 1/\left(3\tau_{total}\right) = \overline{B}/3$.

Spherical Capsule with Continuous Initial Drug Distribution (Both Non-erodible and Erodible Cases)

The prior two sub-sections considered problems in which the sphere, whether erodible or not, has a discrete, layered initial drug distribution. In contrast, the problem of a continuous initial drug distribution, where $\theta_{in}(\xi)$ is a known continuous function of space may also be of interest. Advances in 3D printing may make it possible to print a layered capsule with an initial drug distribution that approximates the desired functional distribution $\theta_{in}(\xi)$. Practical considerations may limit the implementation of spatial variation of θ_{in} to relatively simple functions, since complicated concentration distribution within the capsule may possibly not be accurately reproducible in experiments. Polynomial functions are considered in this section due to their versatility and common usage in fitting experimental data over a finite domain. The solutions of the non-erodible and erodible drug delivery problems remain the same, as given by eq. (11) and (17), respectively, with the expression for the coefficients A_n recast in a more general form as follows for the surface-erodible case

$$A_n = 2\int_0^1 \xi^* \theta_{in}(\xi^*) \sin\left(\lambda_n \xi^*\right) \exp\left(-\frac{\xi^{*2}\overline{B}}{4}\right) d\xi^* \qquad (20)$$

Note that setting $\overline{B} = 0$ in eq. (20) above results in the expression for the non-erodible case.

Moreover, the constraint of maintaining the same total drug mass during optimization, given by eq. (15) for the discrete drug distribution is also written down more generally for both erodible and non-erodible cases as follows

$$\int_0^1 \xi^{*2} \theta_{in}(\xi^*) d\xi^* = \frac{1}{3} \qquad (21)$$

The constraint of non-negative concentration may be written as

$$\theta(\xi) \geq 0 \qquad 0 \leq \xi \leq 1 \qquad (22)$$

Optimization results for the simplest two polynomial functions – linear and quadratic – are discussed, followed by a more general analysis for a polynomial of order J.

Optimization Procedure

An interior-point algorithm [35] solution is utilized to solve the constrained optimization problem summarized in eqs. (14)–(16). To relax the inequality constraints, a vector of slack variables is introduced, and an approximated problem is posed. With this, the optimization problem is then modified using a logarithmic barrier function and the inequalities are removed. For the augmented problem, the optimization iterates are generated using Newton's method, in which, the Jacobian is synthesized using a finite difference routine. The iterations are continued until an appropriate stopping criterion is met. This process is implemented using the '*fmincon*' function in the MATLAB Optimization Toolbox. The tolerances used for the function as well as the constraint satisfaction are set to be 10^{-12}. The minimum allowable step size is also set at 10^{-12}. A local minimum is always found for the range of parameters used. Additionally, the optimization algorithm is initialized with multiple starting values (guesses for the initial concentration), and in all those cases, the results are found to converge to the same values. A more detailed discussion on interior-point optimization methods can be found in [35, 36].

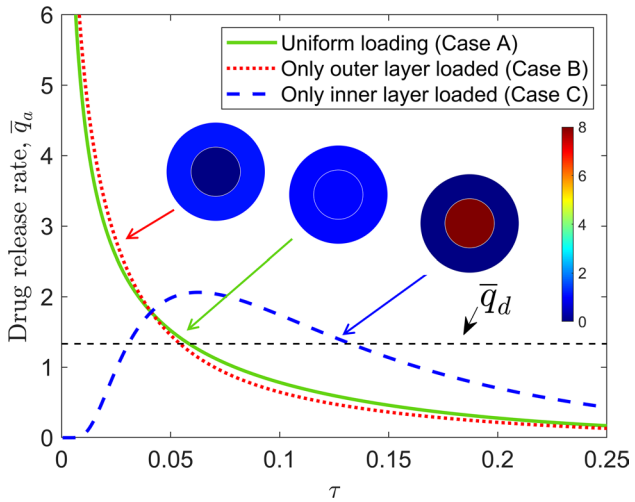

Fig. 2 Drug release rate curves for a non-eroding sphere with two-layered initial drug distribution for three cases – baseline uniform distribution (Case A), drug loaded only in outer layer (Case B) and only in outer layer (Case C). The black dashed line represents the desired constant drug delivery release rate curve. Initial drug concentration distributions for each case are shown as insets.

Results and Discussion

Results for various cases presented in the previous section are now discussed in the same order.

Discrete, Multilayer Drug Cases $\theta_{in,\,m}$

Non-erodible Sphere

The fundamental motivation for optimizing the initial drug distribution in a non-erodible multilayer sphere to obtain a desirable drug release curve is first illustrated. A non-erodible two-layer sphere with radially equidistributed layers (i.e., $\gamma_1 = 0.5$) is considered. Based on a desired constant drug release rate, Fig. 2 plots three candidate designs, including a baseline Case A, in which, both layers have the same initial drug concentration. The other two curves pertain to Cases B and C, in which the entire drug is loaded either in the outer or in the inner layer, respectively, leaving the other layer completely drug-free. The color plots in Fig. 2 represent the initial drug concentration distributions in the layers for each Case. Since drug delivery from the outer surface of the sphere occurs due to a concentration gradient at the surface, for Cases A and B, the rate of drug delivery is very high initially, which then rapidly decays as much of the drug is lost, and the concentration gradient weakens. However, in Case C, since the outer layer does not contain any drug, the initial drug release rate is close to zero, and it grows only slowly before reaching a peak and subsequently decaying. Compared to Cases A and B, the drug release rate curve for Case C, when considered across the time of interest, is relatively flatter, and, in particular, it avoids the large initial drug release. This illustrates the strong dependence of the drug release rate on initial distribution of drug in a multilayer capsule. Even though Case C is an extreme case and not necessarily optimal, its much better performance compared to Cases A and B justifies a systematic optimization in search of the optimal initial drug distribution that produces close to a desired drug release rate.

Several optimization cases are computed for different number of layers in a non-eroding sphere. In each case, the goal is to obtain a constant drug release rate, i.e., based on the non-dimensionalization scheme, $\overline{q}_d(\tau) = 4/3$, while maintaining the total amount of drug loaded to a constant value, per eq. (15). Figure 3(a) presents the optimal drug delivery curves obtained for cases with different number of layers. In each case in Fig. 3, as well as in subsequent Figures, layers are assumed to be radially equidistributed. For comparison, the baseline drug delivery curve for the case with uniform drug distribution throughout the sphere is also shown. The desired drug rate is also shown as a broken line. Figure 3(a) shows that an optimized two-layer sphere already performs much better than the baseline uniformly distributed case in terms of flatness. There is further improvement upon the use of more than two layers, but the incremental improvement is much lower beyond three layers or so. In general, it is not possible to obtain a completely flat curve, even with a large number of layers, due to the constraints imposed by the fundamental nature of diffusion. However, as shown here, optimization can be used to avoid the large initial drug release rate and get as close as possible to a flat curve. Figure 3(b) presents the RMS deviation in the optimized drug distribution as a function of the number of layers. The RMS deviation for the baseline, unoptimized case is also shown as a broken line for comparison. This plot shows a reduction of around 64% in the RMS error in the two-layer

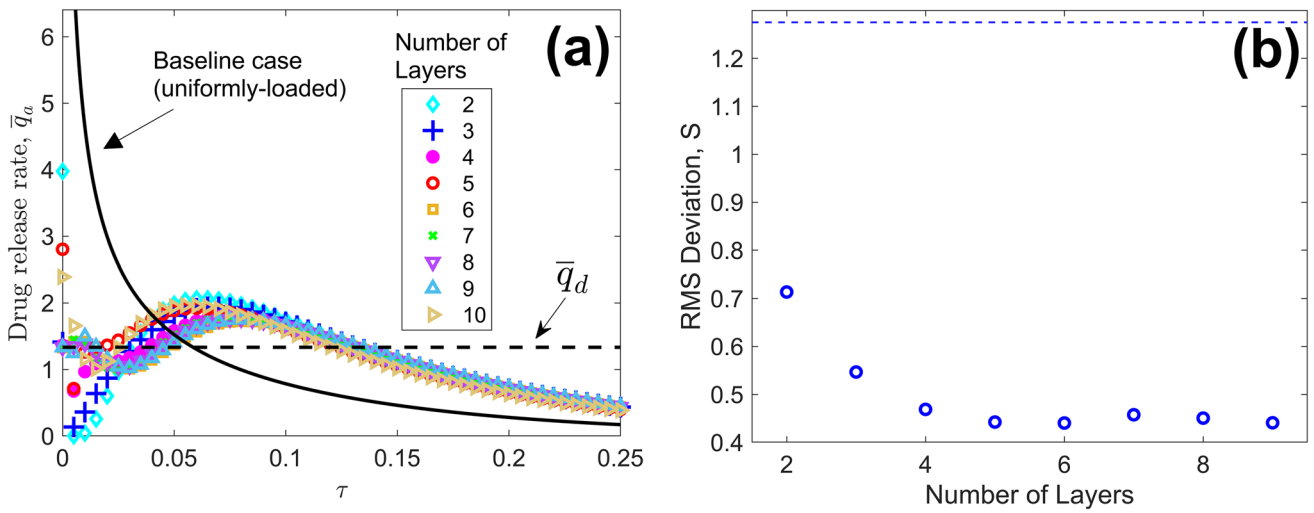

Fig. 3 Optimization results for a non-erodible sphere with initial drug distribution in different number of layers: (a) Optimal drug release rate curves for up to ten-layered sphere, including the curve for the baseline, unoptimized case. The black dashed line represents the desired, constant release rate curve, $\overline{q}_d = \frac{4}{3}$; (b) Minimized RMS deviation (compared to a flat drug release rate curve) as a function of number of layers. RMS error for the baseline, unoptimized case is also shown as a dashed line for comparison.

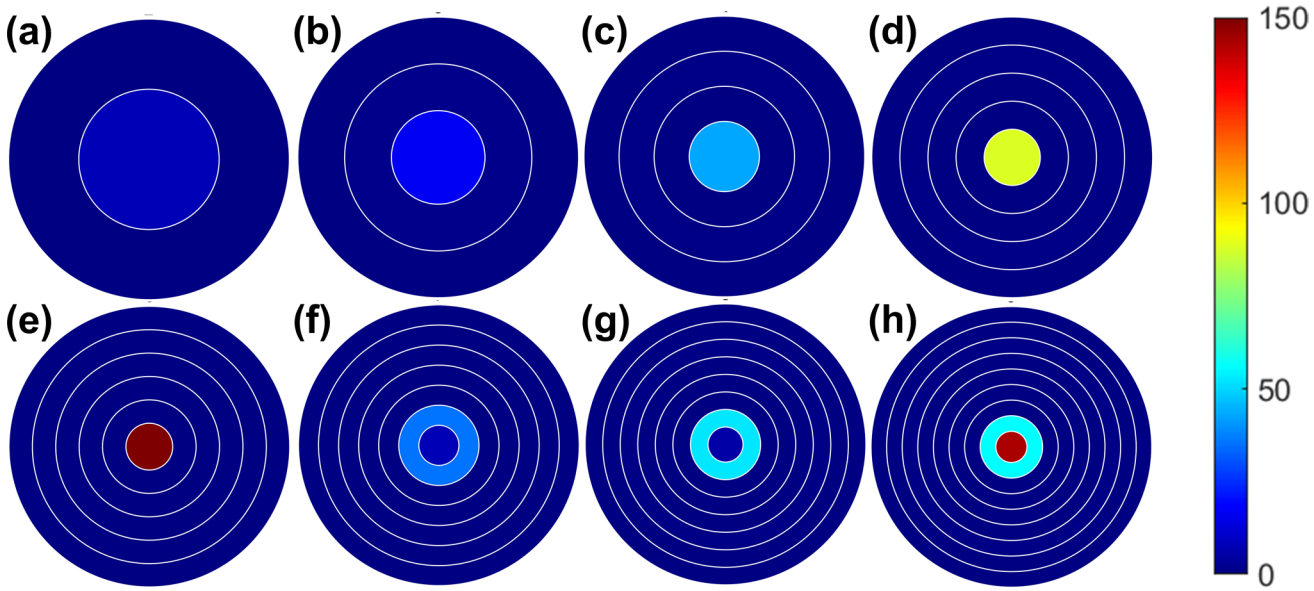

Fig. 4 Color plots of optimized initial drug concentration distributions for the multilayer non-erodible sphere case, for which optimal drug release rate curves are presented in Fig. 3.

case compared to baseline, and further improvement when going to the three-layer case. Beyond that, however, there ceases to be much further improvement. This shows that optimization beyond a few layers may not be worthwhile, especially considering the increased manufacturing cost and complexity due to the additional layers.

It is instructive to examine the optimal drug distributions predicted by the optimization algorithm for different number of layers. These distributions are presented as color plots in Fig. 4, where, in each case, the total mass of drug loaded in the sphere is the same. It is found that in each case, the optimization algorithm focuses on loading most of the drug in the inner layers, while loading no or very little drug in the outer layers. This is consistent with the physical understanding of this problem, wherein, it is critical to reduce the surface concentration gradient at early times to avoid very large rate of drug delivery, for which, it is reasonable that most of the drug be loaded in the inner layers.

For a simple, non-eroding drug delivery device, these results demonstrate the capability of substantial improvement in the nature of drug delivery by optimization of the initial drug distribution in multiple layers. Such information can be valuable for fully maximizing the benefit of manufacturing multilayer drug delivery devices with different drug concentrations in each layer.

Optimization results for a more realistic case of a linearly erodible multilayer sphere is discussed next.

Erodible Sphere

In contrast with the previous sub-section, the results presented here pertain to a sphere that undergoes a linear reduction in its radius. The non-dimensional rate of erosion, defined as $\overline{B} = AB/D$ is an important parameter here. A value of $\overline{B} = 1$, which is representative of several drug delivery scenarios [23] is used. In order to illustrate the importance of optimizing the initial drug distribution for the eroding sphere, results for three Cases of a two-layer erodible sphere are shown in Supplementary Fig. 1. The three cases include baseline case (uniform drug distribution in both layers – Case A), and ones in which all the drug is distributed in the outer layer alone (Case B) or in the inner layer alone (Case C). Similar to Fig. 2 for a non-erodible

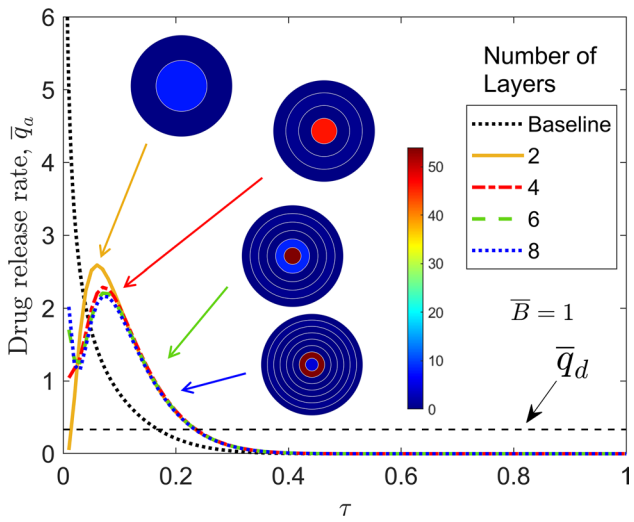

Fig. 5 Optimal drug delivery curves for an eroding sphere ($\overline{B} = 1$) with different number of layers. For reference, the baseline curve for a sphere with uniform drug distribution, as well as the desired constant release rate curve are also shown.

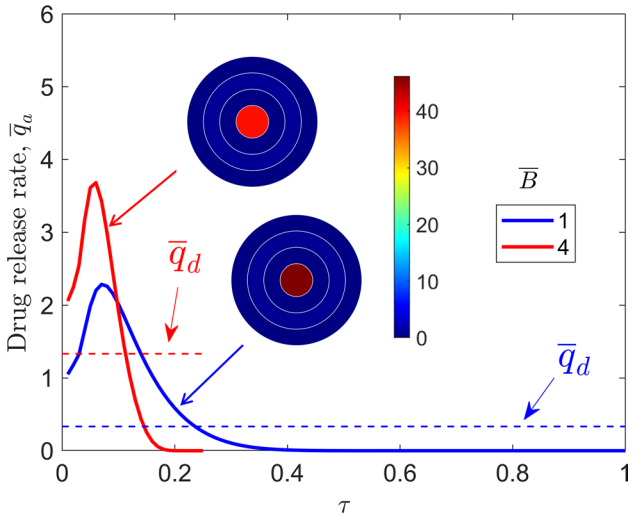

Fig. 6 Comparison of optimal drug delivery curves for two speeds of erosion for an eroding sphere with four layers. For reference, the desirable constant release rate curves for both cases are also shown. The $\overline{B} = 4$ curves end earlier than the $\overline{B} = 1$ curves due to faster erosion of the sphere.

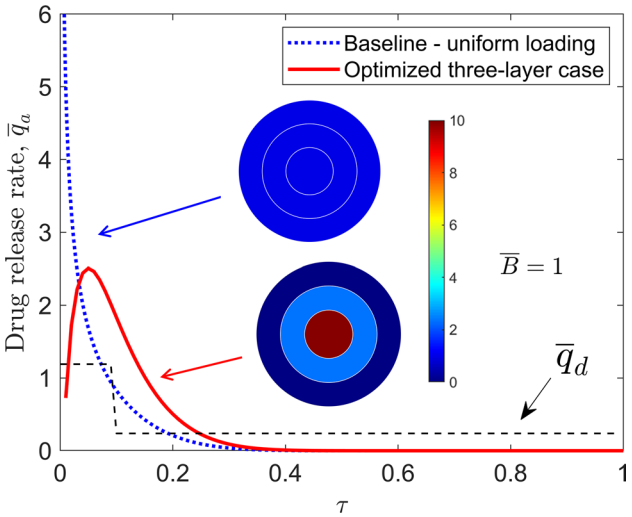

Fig. 7 Demonstration of drug optimization for a case requiring five-fold drug dosage boost in the first 10% of the time period. A three-layer erodible sphere with $\overline{B} = 1$ is considered here.

sphere, this plot shows that loading all the drug in the inner layer (Case C) results in much more uniform drug release rate than the baseline case. Therefore, the motivation to optimize the initial drug delivery distribution is as valid for the erodible case, as it was for the non-erodible case discussed in the previous sub-section.

For a fixed value of the rate of erosion, $\overline{B} = 1$, Fig. 5 plots the optimized initial drug distributions for erodible spheres with four, six and eight layers. A curve corresponding to the baseline case is also plotted. It is seen that as the number of layers increases, the drug release rate gets closer and closer to the ideal flat curve, although, similar to the non-erodible case, the incremental benefit beyond a few layers is relatively minor. The color plots in Fig. 5 illustrate the nature of the optimized drug distributions in each case. In general, the optimization calls for more drug to be distributed in the inner layers, and less in the outer layers. This is similar to the non-erodible case and consistent with the need to reduce surface concentration gradient at small times in order to flatten the drug release rate curve.

Since the non-dimensional rate of erosion is an important problem parameter here, the impact of $\overline{B}$ on the optimization is examined next. Drug delivery optimization is carried out for two different rates of erosion, $\overline{B} = 1$ and $\overline{B} = 4$ for a four-layer device. Keeping the same total amount of drug in each case, Fig. 6 plots the optimized drug delivery curves, as well as the underlying initial drug distributions as color plots. For a surface-erodible sphere, the release time is inversely proportional to the rate of erosion, and therefore, for the $\overline{B} = 4$ case, the drug release process terminates earlier, and therefore, the rate of release is larger. It can be seen from the color plots in Fig. 6 that, in order to meet this elevated drug delivery requirement at early times, the optimization algorithm assigns somewhat greater drug concentration in the outer layers than in the $\overline{B} = 1$ case. As a result, the optimized drug release rate for the $\overline{B} = 4$ case is also elevated, in order to better match the required faster rate of drug delivery over a shorter time. Figure 6 demonstrates the capability of the optimization algorithm to adjust itself to the rate of erosion by assigning an appropriately greater drug concentration in the outer layers.

Erodible Sphere with Initial Burst Release

While all plots presented so far have been based on the goal of obtaining a constant drug release rate, the optimization methodology developed here is quite general, and is applicable to any desired drug release profile. In order to demonstrate this, a case in considered, in which, it is desired to produce an initial burst for a small time, followed by sustained drug release at a constant rate for the remainder time. In order to examine the impact of this desired initial burst on optimal drug distribution, optimization calculations are carried out for a case where a five-fold burst in drug release rate is desired during the first 10% of the time period. For consistency, the same total drug mass is assumed within the sphere as all previous problems. Figure 7 presents the optimized results for this case for a three-layered spherical surface-erodible capsule. The rate of erosion is $\overline{B} = 1$. The drug release rate based on optimized initial drug distribution is plotted in Fig. 7, along with the curve for the baseline case, in which drug is loaded uniformly in all layers. The desired drug release profile, showing a five-fold burst initially, followed by a lower, constant drug release rate is also

shown. Figure 7 shows that with the implementation of the optimized drug distribution in the three layers, shown as a color plot in the inset, the drug release rate curve is much flatter compared to the baseline case. The optimization algorithm assigns most of the drug to the inner-most layer, and relatively lesser drug in the outer layers, resulting in a rate of drug delivery initially that better matches the desired burst. In comparison, the baseline drug release rate is extremely large at the initial time.

The inverse problem defined in this work and the subsequent optimization can be used for any desired drug release rate, and Fig. 7 demonstrates this capability for the specific case of a drug release profile with an initial burst. The initial drug distribution can be similarly optimized for any other desired drug delivery profile that may be highly customized for the needs of a specific patient.

Polynomial Multilayer Drug Distribution $\theta_{in}(\xi)$ (Non-erodible Sphere)

Linear Drug Distribution

A linear initial drug distribution $\theta_{in}(\xi) = \overline{p}_1 + \xi\overline{p}_2$ is considered first. Based on the constraint given by eq. (21), it can be shown that $\overline{p}_2 = \frac{4}{3}\left(1 - \overline{p}_1\right)$, and therefore, $\theta_{in}(\xi) = \left(1 - \frac{4}{3}\xi\right)\overline{p}_1 + \frac{4}{3}\xi$. Therefore, when the initial drug distribution is to be linear, the optimization problem is a one-variable problem. This problem can be analyzed by simply plotting S as a function of $\overline{p}_1$ in the range that satisfies the constraint given by eq. (22), i.e., $0 \le \overline{p}_1 \le 4$. The two extremes within this range, $\overline{p}_1 = 0$ and $\overline{p}_1 = 4$ represent initial drug distribution of $\theta_{in}(\xi) = \frac{4}{3}\xi$ and $\theta_{in}(\xi) = 4(1-\xi)$, respectively. These functions represent a capsule that is heavily loaded towards the outer surface or the center, respectively. Between these two extremes, $\overline{p}_1 = 1$ represents the baseline, uniform drug distribution ($\theta_{in}(\xi) = 1$). Intuitively, in order to make the drug release rate curve as flat as possible, the drug delivery profile must be reduced at early times, and at later times, the curve must be prolonged as much as possible. In order to do so, it is important to reduce drug distribution towards the surface and instead load greater drug concentration near the center.

Figure 8(a) plots RMS deviation of the drug release rate as a function of $\overline{p}_1$ in the feasible range $0 \le \overline{p}_1 \le 4$. Initial drug distributions for three cases – baseline ($\theta_{in}(\xi) = 1$) and two extreme cases, $\theta_{in}(\xi) = \frac{4}{3}\xi$ and $\theta_{in}(\xi) = 4(1-\xi)$ corresponding to $\overline{p}_1 = 0$ and $\overline{p}_1 = 4$, respectively – are also shown in the inset as color plots. Consistent with physical arguments discussed above, S reduces monotonically with increasing $\overline{p}_1$. This shows that, within the given constraints, it is desirable to have as large a value of $\overline{p}_1$ as possible, and therefore $\theta_{in}(\xi) = 4(1-\xi)$ corresponding to $\overline{p}_1 = 4$ is the optimal linear initial drug distribution. The physical interpretation of this result is that an initial drug concentration distribution biased towards the center of the sphere helps reduce the initial peak and prolongs the drug distribution curve. This can be clearly seen in Fig. 8(b), which plots the drug release rate for these three specific cases. For comparison, the desired flat drug release rate curve is also shown as a dotted line. Figure 8(b) shows high mass flux of the drug at early times for each case. However, compared to the baseline, the optimal $\theta_{in}(\xi) = 4(1-\xi)$ case shows a much lower initial peak and a more prolonged flat period before drug delivery goes to zero. This results in a much flatter drug release rate curve than the baseline. The RMS deviation for this case, 0.87, is 58%

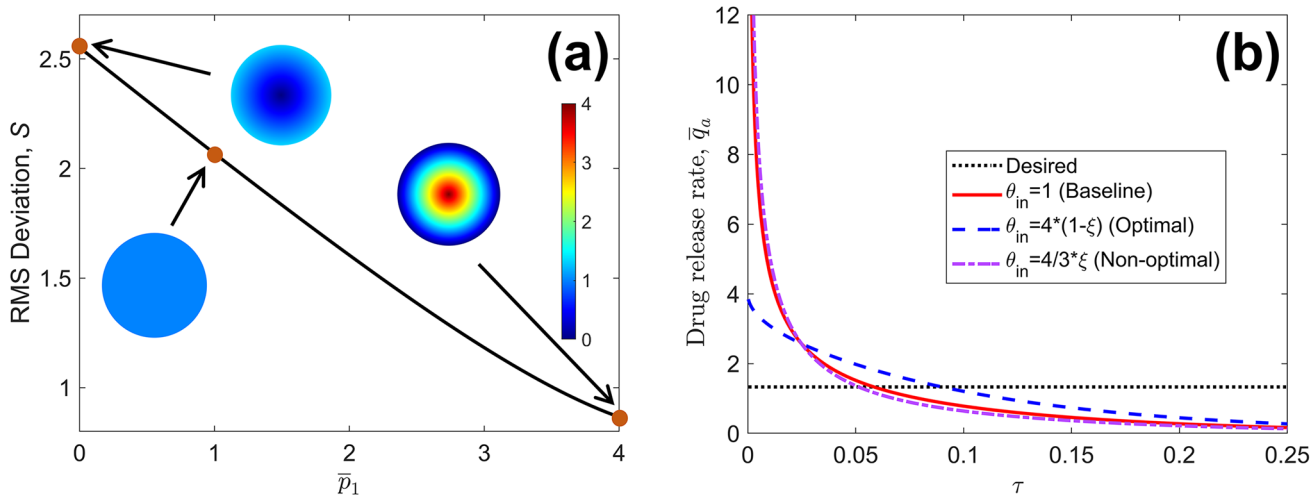

Fig. 8 Optimization results for linear initial drug distribution in a non-erodible sphere: (a) RMS deviation from ideal, flat delivery curve as a function of $\overline{p}_1$, where $\theta_{in}(\xi) = \left(1 - \frac{4}{3}\xi\right)\overline{p}_1 + \frac{4}{3}\xi$. Initial drug distribution curves for three cases – uniform, optimal and non-optimal drug distribution are shown in inset colorplots. (b) Drug delivery curves for the three cases, with the desired constant release rate curve shown for reference.

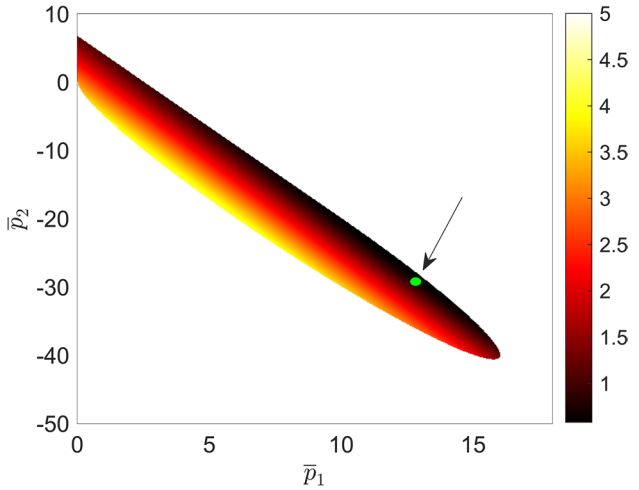

Fig. 9 Colormap showing the RMS deviation from ideal, flat delivery curve in the $\bar{p}_1 - \bar{p}_2$parameter space for quadratic drug distribution in a non-erodible spherical capsule. White space represents the infeasible region where the drug distribution becomes negative at a point within the capsule. While the optimal point is indicated, the dark region shown is also close to optimal.

lower than the baseline value of 2.07, representing a substantial improvement in the uniformity of drug delivery. In contrast, the peak at early times is worse for the non-optimal $\theta_{in}(\xi) = \frac{4}{3}\xi$ case because it loads more drug towards the outer surface, resulting in even greater drug release at early times.

This analysis shows that $\theta_{in}(\xi)=4(1-\xi)$ is the ideal initial linear drug distribution in the spherical capsule. Due to the non-dimensionalization carried out here, this is a universal result that applies to all non-erodible spherical capsules with a linear initial drug distribution.

In search of an even closer drug release rate to that desired, the case of a quadratic initial drug distribution is considered next.

Quadratic Initial Drug Distribution $\theta_{in}(\xi)$

A quadratic initial drug distribution, $\theta_{in}(\xi) = \bar{p}_1 + \xi\bar{p}_2 + \xi^2\bar{p}_3$ facilitates a much larger design space compared to the linear case analyzed in the previous sub-section. In the quadratic case, in order to ensure the same total mass of drug loaded into the capsule, the coefficients in $\theta_{in}(\xi)$ must satisfy $\frac{\bar{p}_1}{3} + \frac{\bar{p}_2}{4} + \frac{\bar{p}_3}{5} = \frac{1}{3}$, so that $\theta_{in}(\xi) = \bar{p}_1 + \xi\bar{p}_2 + 5\xi^2\left(\frac{1}{3} - \frac{\bar{p}_1}{3} - \frac{\bar{p}_2}{4}\right)$ involves two coefficients $\bar{p}_1$ and $\bar{p}_2$ that may be assigned independently. This two-variable optimization problem can be analyzed by plotting the objective function S in the $\bar{p}_1$-$\bar{p}_2$ space and determining the $(\bar{p}_1, \bar{p}_2)$ design point that results in the lowest value of S. Fig. 9 presents a color plot of the objective function S in the $\bar{p}_1$-$\bar{p}_2$ space, shown only in the feasible region that satisfies eq. (16). Fig. 9 shows that, firstly, only a limited region within the two-dimensional $\bar{p}_1$-$\bar{p}_2$ design space is feasible, because for $\bar{p}_1$ and $\bar{p}_2$ values outside this region, the drug distribution becomes negative at one or more points inside the sphere, which is not meaningful in the present work. Within the feasible region, Fig. 9 shows a non-intuitive variation in the RMS deviation as a function of $\bar{p}_1$ and $\bar{p}_2$. In general, there is lower deviation for large positive values of $\bar{p}_1$ and large negative values of $\bar{p}_2$. The optimal point in the $\bar{p}_1$-$\bar{p}_2$ space, in which the RMS deviation is lowest is found to be at $\bar{p}_1 = 13.14$ and $\bar{p}_2 = -29.10$, i.e., a quadratic drug distribution of $\theta_{in}(\xi) = 13.14 - 29.10\xi + 16.14\xi^2$. Figure 10(a) presents drug release rate curves for the baseline and optimal cases. Two additional cases – a near-optimal quadratic case, $\theta_{in}(\xi) = 10 - 20\xi + 10\xi^2$ and the optimal linear case $\theta_{in}(\xi)=4(1-\xi)$ – are also shown for comparison. Figure 10(a) shows a much flatter drug release rate curve for the optimal quadratic case. The RMS deviation is 0.58 compared to 2.07 for the baseline case, representing a reduction of around 72%. In comparison, the corresponding RMS deviation for the optimal

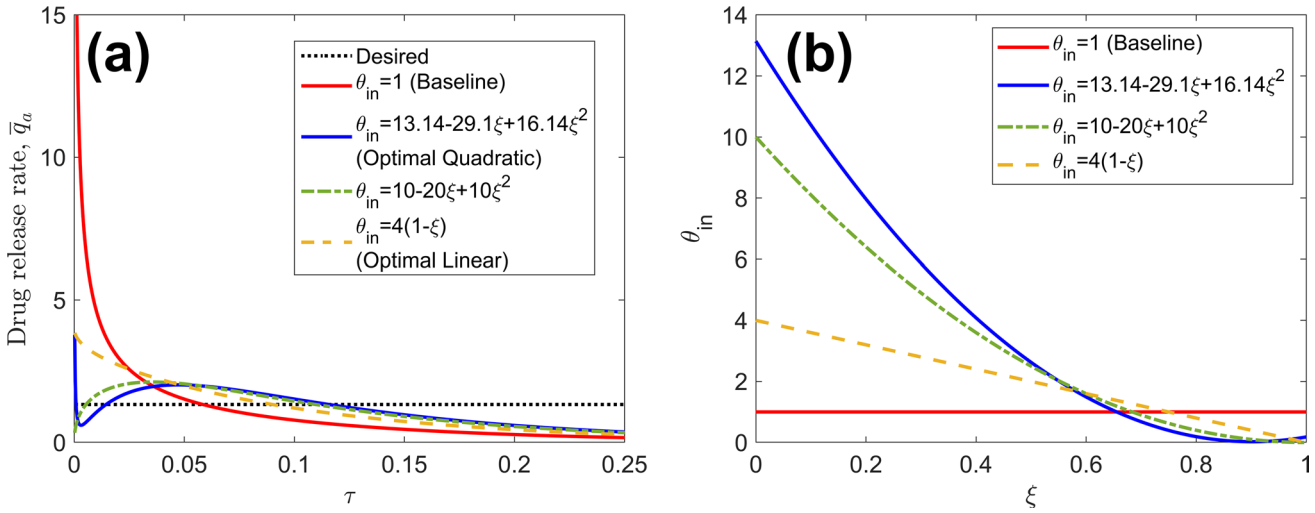

Fig. 10 Optimized results for non-erodible spherical capsule with quadratic drug distribution: (a) Drug delivery curve for a number of quadratic drug distributions. The desired constant release rate curve and optimized linear curve are also shown for comparison‘(b) Initial drug distribution curves for the cases plotted in part (a).

linear case is 0.87. Compared to the baseline case, the rate of drug delivered at initial times is much lower for the optimal case. Additionally, while the mass flux goes down monotonically for the baseline case, it reduces, then increases and finally reduces in the optimal case, all the while staying much closer to the desired flat curve.

An interesting aspect of the variation of RMS deviation in the $\overline{p}_1$-$\overline{p}_2$ space is that the RMS surface around the minima, found at $\overline{p}_1 = 13.14$ and $\overline{p}_2 = -29.10$, is rather flat. Therefore, there is a reasonably large region in the $\overline{p}_1$ -$\overline{p}_2$ plane, where the RMS deviation is quite close to the minimum value. For example, for $\theta_{in}(\xi) = 10 - 20\xi + 10\xi^2$ plotted in Fig. 10(a), the RMS deviation is 0.61, which is within 5% of the optimal case. Therefore, it may be possible for a drug designer to choose within a greater design space without sacrificing much in terms of the drug release rate.

Figure 10(b) illustrates the nature of drug distribution curves within the sphere for the cases considered here. While the baseline curve is flat, corresponding to uniform drug distribution, the optimal drug distribution curve starts very high at the center and has a minima of zero concentration just before the outer surface of the capsule. For comparison, drug distributions for the optimal linear and nearly-optimal quadratic cases shown in Fig. 10(a) are also plotted here. Both of these curves are monotonic and reduce to zero concentration at the surface. In case implementing the optimal drug distribution, with a minimum, zero concentration close to the surface is experimentally challenging, one may adopt a monotonic curve, such as $\theta_{in}(\xi) = 10 - 20\xi + 10\xi^2$, without much loss of performance.

General Polynomial Initial Drug Distribution $\theta_{in}(\xi)$

A general polynomial initial drug distribution is now considered, i.e., $\theta_{in}(\xi) = \sum_{j=0}^{J} \overline{p}_{j+1}\xi^j$, where J is the degree of the polynomial. In this case, the design space is much larger, and a brute force search for the optimal, similar to linear and quadratic distributions in the previous subsection is no longer possible. Inserting the general J-order polynomial form into the mass conservation requirement eliminates one of the coefficients, and therefore, this is a problem of J-parameter optimization, defined by eqs. (14), (16) and the following form of eq. (15) written for the assumed polynomial form

$$\text{subject to} \quad \sum_{j=0}^{J} \frac{\overline{p}_{j+1}}{j+3} = \frac{1}{3} \tag{23}$$

Similar to the multilayer sphere cases, optimization for this case is carried out using the procedure outlined previously. Representative optimization results for this case are presented in Fig. 11. The optimized drug release rates are plotted for polynomials of degrees 1 (linear) through 6 in Fig. 11(a). The RMS deviation S is also plotted as a function of the degree of polynomial in Fig. 11(b). These plots show substantial improvement in the drug delivery for the $J=1$ (linear) and $J=2$ (quadratic) cases compared to baseline. Beyond these cases, the drug release rate curves in Fig. 11(a) are nearly identical, and correspondingly, the values of RMS deviation plateau out, as shown in Fig. 11(b). This shows, similar to the plots for the discrete multilayer case, that the benefit of optimizing the initial dug distribution reaches a plateau, and there is not much additional benefit in considering increasingly complex initial drug distributions. Such insights must be carefully considered along with cost and complexity in order to determine the best initial drug distribution.

Note that while results in this section are presented in the context of a polynomial form of the initial drug distribution,

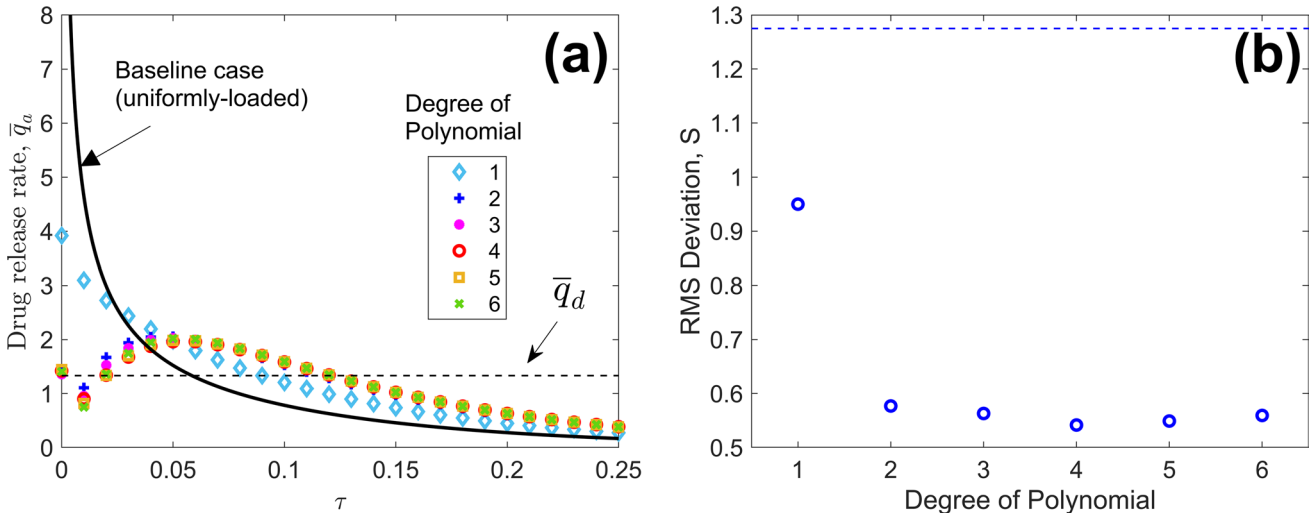

Fig. 11 Optimized drug delivery curves for a non-erodible spherical capsule with polynomial drug distributions of different degrees; (b) Minimized RMS error as a function of degree of polynomial.

the optimization framework utilized here is a general one, and it is possible to optimize based on initial drug distributions of other forms, such as power functions or exponential functions instead of polynomials.

Conclusions

The key contribution of the present work is in optimizing the initial drug distribution in a multilayer surface-erodible spherical capsule for attaining a desired drug release rate over time. A key conclusion of the results discussed here is that while there is substantial early stage improvement, for example, for a two- or three-layered capsule, the incremental benefit in considering more complicated systems, such as a capsule with more than three layers, is rather limited.

By solving the forward problem and carrying out optimization in non-dimensional form, this work ensures universal applicability of the results. For example, the results for the non-erodible sphere are applicable for a sphere of any dimension, as long as the underlying assumptions are satisfied. Similarly, results for the erodible sphere case are also universally applicable, with the non-dimensional rate of erosion as the key parameter.

It is important to recognize the key limitations of the present work. Dissolution is assumed to occur rapidly. If dissolution was to be the rate-limiting factor, then the qualitative trends reported here would still be valid. However, the overall timescale for drug to be released would increase, in a manner dependent on the specific dissolution properties of the drug within the delivery system. The diffusion coefficient is assumed to be invariant during the drug delivery process and the outer boundary is modeled in terms of a zero concentration boundary, although this can be easily extended to account for non-sink conditions. These assumptions are reasonable for a broad range of drug delivery problems. The theoretical model presented here does not consider the possibility of API-excipient interactions, which may alter the drug release rate, and may also not be appropriate when considering complex systems such as Amorphous Solid Dispersions (ASDs). In general, however, the optimization algorithm can be easily extended to account for additional effects, as long as the forward problem can be readily solved.

While presented in the context of uniform drug delivery curves and those with an initial burst, the methodology presented here can be easily extended to other drug delivery requirements as well. It is expected that the methodology and results presented in this work may be helpful in maximizing the benefit of advanced manufacturing technologies capable of producing multilayer drug delivery devices that address the individualized drug delivery needs of patients. To help facilitate this, it is hoped that this work will inspire future experiments to fully validate the model and test model predictions of optimal drug distribution for different applications.

Supplementary Information The online version contains supplementary material available at https://doi.org/10.1007/s11095-022-03359-y.

Author Contributions A. Jain – Conceptualization, Methodology, Formal Analysis, Validation, Investigation, Data Curation, Project Administration; K. Subbarao – Formal Analysis, Validation, Investigation, Data Curation; S. McGinty – Methodology, Formal Analysis, Validation; G. Pontrelli – Methodology, Formal Analysis, Validation. All authors contributed towards Writing Original Draft, Review and Editing.

Funding Funding from the European Research Council under the European Unions Horizon 2020 Framework Programme (No. FP/2014 \ 0552020)/ ERC Grant Agreement No. 739964 (COPMAT) is acknowledged. This work is also partially supported by Italian MIUR (PRIN 2017 project: Mathematics of active materials: from mechanobiology to smart devices, # 2017KL4EF3).

Data Availability The datasets generated during and/or analysed during the current study are available from the corresponding author on reasonable request.

Declarations

Conflict of Interest The authors declare that they do not have any conflicts of interest in connection with this work.

References

1. Siepmann J, Siepmann F. Mathematical modelling of drug delivery. Int J Pharm. 2008;364:328–43. https://doi.org/10.1016/j.ijpharm.2008.09.004.
2. Stefanini GG, Holmes DR. Drug-eluting coronary artery stents. N Engl J Med. 2013;368:254–65. https://doi.org/10.1056/NEJMra1210816.
3. Prausnitz MR, Langer R. Transdermal drug delivery. Nat Biotechnol. 2008;26:1261–8. https://doi.org/10.1038/nbt.1504.
4. Liechty WB, Kryscio DR, Slaughter BV, Peppas NA. Polymers for drug delivery systems. Annu Rev Chem Biomolec Eng. 2010;1:149–73. https://doi.org/10.1146/annurev-chembioeng-073009-100847.
5. Tarcha P. Polymers for controlled drug delivery. 1st ed: CRC Press; 1990.
6. Jain A, McGinty S, Pontrelli G, Zhou L. Theoretical model for diffusion-reaction based drug delivery from a multilayer spherical capsule. Int J Heat Mass Transf. 2022;183:122072:1-14. https://doi.org/10.1016/j.ijheatmasstransfer.2021.122072.
7. Laracuente M-L, Yu M, McHugh K. Zero-order drug delivery: state of the art and future prospects. J Control Release. 2020;327:834–56. https://doi.org/10.1016/j.jconrel.2020.09.020.
8. Bruschi ML. Mathematical models of drug release. Woodhead Publishing. 2015:63–86. https://doi.org/10.1016/B978-0-08-100092-2.00005-9.
9. Dekyndt B, Verin J, Neut C, Siepmann F, Siepmann J. How to easily provide zero order release of freely soluble drugs from coated pellets. Int J Pharm. 2015;478:31–8. https://doi.org/10.1016/j.ijpharm.2014.10.071.

10. Tzafriri AR, Groothuis A, Price GS, Edelman ER. Stent elution rate determines drug deposition and receptor-mediated effects. J Control Release. 2012;161:918–26. https://doi.org/10.1016/j.jconrel.2012.05.039.
11. Eyjolfsson, R., 'Design and manufacture of pharmaceutical tablets,' 1st Ed., Elsevier, 2014. ISBN: 9780128021828.
12. Vaithiyalingam SR, Sayeed VA. Critical factors in manufacturing multi-layer tablets—assessing material attributes, in-process controls, manufacturing process and product performance. Int J Pharm. 2010;398:9–13. https://doi.org/10.1016/j.ijpharm.2010.07.025.
13. Abebe A, Akseli I, Sprockel O, Kottala N, Cuitiño AM. Review of bilayer tablet technology. Int J Pharm. 2014;461:549–58. https://doi.org/10.1016/j.ijpharm.2013.12.028.
14. Goyanes A, Fina F, Martorana A, Sedough D, Gaisford S, Basit AW. Development of modified release 3D printed tablets (printlets) with pharmaceutical excipients using additive manufacturing. Int J Pharm. 2014;527:21–30. https://doi.org/10.1016/j.ijpharm.2017.05.021.
15. Fina F, Madla CM, Goyanes A, Zhang J, Gaisford S, Basit AW. Fabricating 3D printed orally disintegrating printlets using selective laser sintering. Int J Pharm. 2018;541:101–7. https://doi.org/10.1016/j.ijpharm.2018.02.015.
16. Karakurt I, Aydoğdu A, Çıkrıkcı S, Orozco J, Lin L. Stereolithography (SLA) 3D printing of ascorbic acid loaded hydrogels: a controlled release study. Int J Pharm. 2020;584:119428. https://doi.org/10.1016/j.ijpharm.2020.119428.
17. Karalia D, Siamidi A, Karalis V, Vlachou M. 3D-printed Oral dosage forms: Mechanical properties, computational approaches and applications. Pharmaceutics. 2021;13:1401:1-37. https://doi.org/10.3390/pharmaceutics13091401.
18. Vergnaud J-M. Controlled drug release of oral dosage forms. Boca Raton, FL: CRC Press; 2009.
19. Arifin DY, Lee LY, Wang C-H. Mathematical modeling and simulation of drug release from microspheres: Implications to drug delivery systems. Adv Drug Deliv Rev. 2006;58:1274–325. https://doi.org/10.1016/j.addr.2006.09.007.
20. Crank J. The mathematics of diffusion. 2nd ed: Oxford Science Publications; 1980.
21. Jain A, McGinty S, Pontrelli G, Zhou L. Theoretical modeling of endovascular drug delivery into a multilayer Arterial Wall from a drug-coated balloon. Int J Heat Mass Transf. 2022;187:122572. https://doi.org/10.1016/j.ijheatmasstransfer.2022.122572.
22. d'Errico M, Sammarco P, Vairo G. Analytical modeling of drug dynamics induced by eluting stents in the coronary multi-layered curved domain. Math Biosci. 2015;267:79–96. https://doi.org/10.1016/j.mbs.2015.06.016.
23. Jain A, McGinty S, Pontrelli G. Drug diffusion and release from a bioerodible spherical capsule. Int J Pharm. 2022;616:121442. https://doi.org/10.1016/j.ijpharm.2021.121442.
24. Zhang M, Yang Z, Chow L-L, Wang C-H. Simulation of drug release from biodegradable polymeric microspheres with bulk and surface erosions. J Pharm Sci. 2003;92:2040–56. https://doi.org/10.1002/jps.10463.
25. Harland RS, Dubernet C, Benoit J-P, Peppas NA. A model of dissolution-controlled, diffusional drug release from non-swellable polymeric microspheres. J Control Release. 1988;7:207–15. https://doi.org/10.1016/0168-3659(88)90053-3.
26. Sundararaj SC, Thomas MV, Dziubla TD, Puleo DA. Bioerodible system for sequential release of multiple drugs. Acta Biomater. 2014;10:115–25. https://doi.org/10.1016/j.actbio.2013.09.031.
27. McGinty S, Pontrelli G. On the role of specific drug binding in modelling arterial eluting stents. J Math Chem. 2016;54:967–76. https://doi.org/10.1007/s10910-016-0618-7.
28. Özişik MN. Inverse heat transfer: fundamentals and applications. 1st ed. Routledge; 2000.
29. Lee PI. Initial concentration distribution as a mechanism for regulating drug release from diffusion controlled and surface erosion controlled matrix systems. J Control Release. 1986;4:1–7. https://doi.org/10.1016/0168-3659(86)90027-1.
30. Nauman EB, Patel K, Karande P. On the design and optimization of diffusion-controlled, planar delivery devices. Chem Eng Sci. 2010;65:923–30. https://doi.org/10.1016/j.ces.2009.09.043.
31. Georgiadis MC, Kostoglou M. On the optimization of drug release from multi-laminated polymer matrix devices. J Control Release. 2001;77:273–85. https://doi.org/10.1016/s0168-3659(01)00510-7.
32. Lu S, Ramirez F, Anseth KS. Modeling and optimization of drug release from laminated polymer matrix devices. AICHE J. 1998;44:1689–96. https://doi.org/10.1002/aic.690440720.
33. Larobina D, Mensitieri G, Kipper M, Narasimhan B. Mechanistic understanding of degradation in bioerodible polymers for drug delivery. AICHE J. 2002;48:2960–70. https://doi.org/10.1002/aic.690481221.
34. Wong HM, Wang JJ, Wang CH. In vitro release of human immunoglobulin G from biodegradable microspheres. Ind Eng Chem Res. 2001;40:933–48. https://doi.org/10.1021/ie0006256.
35. Nocedal J, Wright S Numerical optimization. Berlin/Heidelberg: Springer Science & Business Media; 2006.
36. Boyd S, Vandenberghe L. Convex optimization. Cambridge: Cambridge University Press; 2004.